PARAMETRIC ROTOR CONTROL EQUIVALENT TURBULENCE INPUT (RCETI) MODELS USING NEURAL NETWORKS

Mahmoud A. Hayajnh
School of Aerospace Engineering
Georgia Institute of Technology
Atlanta, Georgia, USA

J.V.R. Prasad
School of Aerospace Engineering
Georgia Institute of Technology
Atlanta, Georgia, USA

ABSTRACT

This paper extends the concept of Rotor Control Equivalent Turbulence Input (RCETI) to simulate the response of various rotor configurations to two-dimensional spatial turbulence, with the aim of developing parametric RCETI models. Using CIFER®, transfer functions were constructed to match the Power Spectral Density (PSD) of required inputs, effectively replicating the rotor response to turbulence. Unlike previous studies, this work encompasses a broader range of rotor parameters and employs non-dimensional parameters to study the generalizability of the model. Additionally, neural network modeling is utilized to create parametric models, with non-dimensional rotor parameters as inputs and RCETI model parameters as outputs. The study demonstrates that these parametric RCETI models can be effectively developed using a simple neural network architecture, which also shows scalability to different rotor configurations.

NOTATION

Y	Output
U	Input
G	Transfer function
S_x	Auto-Power Spectral Density of signal x
w_g	Turbulence vertical velocity, ft/s
U_0	Mean wind speed, ft/s
L_w	Vertical turbulence scale length, ft
C_T	Thrust coefficient
C_{M_y}	Rotor hub pitch moment coefficient
C_{M_x}	Rotor hub roll moment coefficient
J	Fit error function
$\hat{T}_c$	Frequency response from CIFER
T	Frequency response from transfer function
N_b	Number of rotor blades
c	Blade chord length, ft
r	Radial location on blade, ft
R	Rotor radius, ft
e	Flapping hinge offset, % of R
s	Laplace variable
ω	Temporal frequency, rad/s
Ω_1, Ω_2	Spatial frequency, rad/ft
Φ	Uniformly distributed phase angle, rad
σ_w	Vertical turbulence intensity, ft/s
θ_0	Swash-plate collective angle, deg
θ_{1s}	Swash-plate longitudinal angle, deg
θ_{1c}	Swash-plate lateral angle, deg
CETI	Control Equivalent Turbulence Input
RCETI	Rotor Control Equivalent Turbulence Input
PSD	Power Spectral Density
LHS	Latin Hybercube Sampling

INTRODUCTION

Rotorcraft are complex machines that utilize rotating blades or rotors to generate lift and propulsion. They have a unique ability to take off and land vertically, making them ideal for applications such as search and rescue, transportation, firefighting, and military operations. However, rotorcraft are particularly sensitive to changes in airflow due to their vertical lift capability, making turbulence modeling and simulation crucial for evaluating their ability to perform tasks in adverse weather conditions.

The traditional approach to model the effect of turbulence on vehicles is done by assuming that the aircraft velocity is much higher than the turbulence velocity, and thus, a spatially frozen-field pattern of body axis gust velocities is generated from, for example, Von Karman or Dryden turbulence models (Ref. 1) and are summed into the aircraft equations of motion. An improved approach by the implementation of complex rotating frame turbulence models (Ref. 2) was found to be applicable for low speed/hover tasks. However, these approaches to modeling turbulence are primarily intended for simulation purposes and cannot be utilized for in-flight simulation or testing (Ref. 3). This is because they are integrated into the aircraft equations of motion and require a nonlinear aircraft model with blade element representation. Therefore, while these modeling approaches are valuable tools for vehicle control design and development, they cannot completely replace in-flight testing for verifying the performance of a vehicle in turbulent conditions (Ref. 2).

The notion of using control inputs that result in vehicle response that is stochastically similar to its response to atmospheric turbulence has been identified to reduce *in situ* flight testing, thus reducing risk during vehicle and its control system development. This approach was first put forward by the National Research Council (NCR), Canada (Ref. 4). The angular rates and vertical accelerations from data of the Bell 205 hovering in turbulence were processed via a first-order inverse model of the aircraft to obtain input traces. These traces were then used as inputs to the aircraft actuators, yielding a response similar to the one measured from flight in turbulence. This notion was later extensively studied by the US Army Aeroflightdynamics Directorate (AFDD) at NASA Ames, which resulted in the development of the Control Equivalent Turbulence Input (CETI) models (Refs. 3,5,6). In the CETI approach, the control inputs required to drive the vehicle response to become stochastically similar to the response in actual turbulence are determined. The CETI model for the UH-60 helicopter was developed using vehicle responses from flight tests in turbulence. The method was later applied to the EC135 helicopter at the German Aerospace Center (DLR) (Ref. 7), showing that the approach can be applied to different aircraft.

In spite of these and similar successes of the CETI method (Refs. 8–11), the applicability of the derived CETI models to vehicles other than those used in their development is still an open question. An Achilles heel in the generalization of CETI models that are scalable across small UAS to large size rotorcraft is the large parameter space involved in the development of generic models that are applicable across different vehicle types, number of rotors, and their arrangement. Thus, this research builds on the previous studies that developed turbulence models for specific helicopters. The aim here, however, is to focus on the rotor and develop an equivalent control input for the rotor which results in hub load responses stochastically similar to responses due to turbulence. This recognizes that, at low speeds, the stochastic characterization of vehicle response to turbulence is very largely driven by stochastic characterization of rotor hub loads. As a result, the Rotor Control Equivalent Turbulence Input (RCETI) models are developed, which in turn narrows the parameter space for RCETI model generalization to rotor-specific parameters. Earlier work has demonstrated that RCETI models can effectively mimic rotorcraft responses to atmospheric turbulence, as applied to the UH-60 helicopter (Ref. 12). Initial efforts in this direction have also confirmed the feasibility of creating parametric models that can be adapted and scaled based on different rotor parameters, such as chord length and number of blades (Ref. 13). Later on, the extension and application of RCETI models to multi-rotor platforms have been explored, exemplified through the application to a quadrotor vehicle (Ref. 14).

Therefore, the primary objective of the current study is to broaden the scope of rotor parameters examined in developing parametric Rotor Control Equivalent Turbulence Input (RCETI) models. Specifically, this research aims to incorporate an extensive number of rotor parameters to present the methodology of developing parametric RCETI models, including different non-dimensional parameters of rotors. By doing so, the study provides a proof of concept that demonstrates the potential for these models to be extended and scaled for various rotorcraft configurations. Furthermore, a Neural Network architecture is utilized to fit the model, with the non-dimensional parameters as inputs and the RCETI filter parameters as outputs.

METHODOLOGY

As discussed in the introduction, developing models for turbulence simulation is a challenging task that has been the focus of extensive research. The Control Equivalent Turbulence Input (CETI) models have emerged as a viable approach to incorporate the influence of turbulence. These models aim to capture the impact of turbulence using control inputs, enabling a direct and efficient approach to assess the response and performance of vehicles in turbulent conditions.

Control Equivalent Turbulence Input (CETI) models

The development of Control Equivalent Turbulence Input (CETI) models has been approached through various methodologies. The CETI model developed previously (Ref. 6) used a combined frequency and time-domain approach. This method involved analyzing the remnant input time histories in the frequency-domain to determine the CETI model parameters. This combined method requires the development of a stabilized inverse of the identified aircraft model to perform the inverse time-domain simulation. Similar approaches have been employed in other investigations (Refs. 7, 15). Recently, a frequency-domain approach was proposed and used to develop the CETI model (Refs. 9, 16), which did not require an

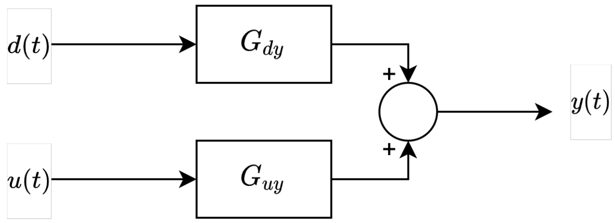

Figure 1. Vehicle response to both input and turbulence

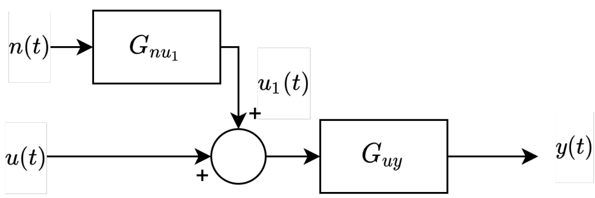

Figure 2. Block diagram of control equivalent turbulence input model.

inverse aircraft model. This approach is considered in the following discussion and the methodology is described.

Consider the block diagram shown in Fig. 1, the SISO equation for this diagram can be written in the frequency domain as:

$$Y(\omega) = G_{uy}(\omega)U(\omega) + G_{dy}(\omega)D(\omega) \tag{1}$$

where G_{uy} represents the aircraft response to input u, and G_{dy} represents the aircraft response to turbulence d.

The equation for the system with the block diagram in Fig. 2 is:

$$Y(\omega) = G_{uy}(\omega)[U(\omega) + U_1(\omega)] \tag{2}$$

where U_1 represents the remnant input that is used to account for the aircraft response to turbulence. By rearranging Eq. (2), to solve for the remnant input U_1:

$$U_1(\omega) = \frac{1}{G_{uy}(\omega)} Y(\omega) - U(\omega) \tag{3}$$

The power spectral density (PSD) of the remnant input ($S_{u_1u_1}$) is defined as follows (Ref. 17):

$$S_{u_1u_1}(\omega) = \lim_{T\to\infty} \frac{1}{T}\{U_1^* U_1\} \tag{4}$$

And the magnitude of the CETI transfer function model G_{nu_1} is then found when driven by a unity PSD white noise input as:

$$|G_{nu_1}| = \sqrt{S_{u_1u_1}} \tag{5}$$

A CETI transfer function can then be identified via frequency domain system identification techniques such as CIFER® (Ref. 18).

Rotor Control Equivalent Turbulence Input (RCETI) models

The spectra of the aircraft rates were the basis of earlier efforts to create the CETI models. In order to reduce the number of parameters for the generalization of such models, the fixed system hub-loads comprising rotor thrust, pitch moment, and roll moment may be considered. The stochastic characterization of vehicle response to turbulence is very largely driven by the stochastic characterization of rotor hub loads. Hence, the RCETI methodology is aimed at finding rotor control inputs that result in hub loads stochastically similar to those due to atmospheric turbulence (see Fig. 3). Since this modeling framework is rotor specific, parametric studies covering different rotors and rotor parameters can be carried out to develop a parametric RCETI model.

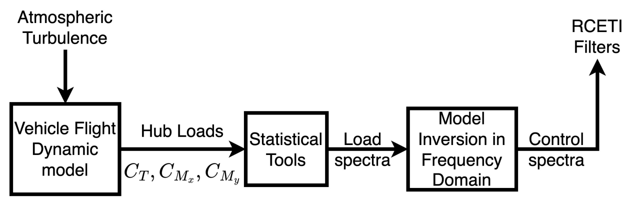

Figure 3. Rotor Control Equivalent Turbulence Input (RCETI) Modeling Framework.

For example, as a SISO case, the spectrum of the thrust coefficient (C_T) as output due to turbulence can be found as follows:

$$S_{C_T}(\omega) = \lim_{T\to\infty} \frac{1}{T}\{C_T^* C_T\} \tag{6}$$

Next, an inverse mapping of the load spectrum to rotor control spectrum comprising collective (θ_0) control can be developed. This can be found in the frequency domain by the following equation:

$$S_{\theta_0}(\omega) = |G_{\theta_0 C_T}(\omega)|^{-2} S_{C_T}(\omega) \tag{7}$$

At this point, the RCETI models are formed by converting the control spectrum to a parametric filter transfer function via frequency domain system identification techniques using CIFER®.

Parametric RCETI models

The analysis can then be extended to varying rotor parameters, wherein the rotor parameters can be modified to develop different RCETI models (*i.e.,* the analysis in Fig. 3 is repeated for different rotor parameters). The effect of changing rotor parameters on the Rotor Control Equivalent Turbulence Input (RCETI) models can then be investigated. This work has been proposed, and the analysis has been carried out for varying rotor parameters such as chord length, number of blades, and rotor radius (Ref. 13). A conventional single main rotor helicopter model was used in the analysis and the parameters were altered to asses the impact of change of these parameters on the shape and characteristics of the PSD of the RCETI models. Since it has been shown that the rotor is the main load-producing element of the vehicle in turbulence, this study focuses on isolated rotors.

Selection of Dimensional and Non-Dimensional Parameters

In this study, the choice of both dimensional and non-dimensional parameters was guided by their impact on the aerodynamic and dynamic response of rotor. The primary focus was on the main rotor parameters, which were selected as the design parameters due to their critical role in governing the behavior of the rotorcraft.

Dimensional Parameters The dimensional parameters selected and their effect on the non-dimensional parameters is described bellow:

- **Chord Length (c):** The chord length influences the lift generation and aerodynamic loading on the rotor blades. It directly changes the solidity and the lock number.
- **Number of Blades (N_b):** The number of blades in the rotor system affects the dynamic response as well as the harmonic content of the rotor response.
- **Rotor Radius (R):** The rotor radius defines the rotor disk area, which directly affects the overall thrust produced by the rotor.
- **Nominal Rotational Speed (Ω):** The rotational speed of the rotor is a key factor in determining the rotor tip speed which affects the aerodynamic response of the rotor.
- **Blade Second Moment of Inertia (I_B):** This parameter is related to the inertial force of the blade, and is directly influencing the lock number.
- **Flapping Hinge Offset (e):** The hinge offset affects the flapping motion of the rotor blades, influencing both the aerodynamic forces and moments and the dynamic stability of the rotor.
- **Nominal Weight/Thrust (W):** This changes the nominal trim thrust coefficient required to be produced by the rotor.

Non-Dimensional Parameters The non-dimensional parameters derived from the dimensional ones include:

- **Solidity (σ):** Solidity is the ratio of the total rotor blade area to the rotor disk area.
- **Lock Number (γ):** The Lock number characterizes the relationship between the aerodynamic forces and the inertia of the rotor blades, playing a crucial role in the dynamic behavior of the rotor system.
- **Tip Mach number (M_{Tip})** This parameter represents the tip speed of the rotor blades relative to the speed of sound, which is essential in determining the aerodynamic efficiency and potential for compressibility effects.
- **Thrust Coefficient (C_T):** The thrust coefficient is a non-dimensional measure of the rotor thrust relative to the rotor disk area and the dynamic pressure, providing insight into the rotor aerodynamic performance.
- **Flapping Frequency (ν):** This parameter describes the frequency of the flapping motion of the rotor blades, affecting the dynamic response of the rotor.

These non-dimensional parameters are chosen because they cover the essential aerodynamic and dynamic characteristics of the rotor system. By considering the aforementioned dimensional and non-dimensional parameters, this research ensures a comprehensive list for the study of developing parametric RCETI models.

RESULTS

In previous studies (Refs. 12, 13), the analysis focused on studying the use RCETI models instead of the CETI models to replicate the vehicle response to turbulence. The PSD of rotor and vehicle response to turbulence is found and compared to show that rotors are the main load-producing elements in turbulence. The hub-fixed sampling of turbulence was considered. In addition, the effect of the longitudinal and lateral spatial gradients of the vertical turbulence ($\frac{\partial w_g}{\partial x}$ and $\frac{\partial w_g}{\partial y}$) was included. Both CETI and RCETI models, for a representative model of the UH-60 Helicopter, have been developed and compared. A parametric study was carried out for limited number of rotor parameters. In Ref. 19, the integration of the two-dimensional turbulence model was considered, allowing for the rotational sampling effect of turbulence.

In this paper, we consider the development of RCETI models for an isolated rotor to replicate the two-dimensional spectrum of turbulence for different rotor configurations. The results from the different configurations are used to develop a Neural Network for the parametric RCETI model. This Neural Network can later be used to construct the RCETI model for other rotor parameters which were not used in the training of the network.

FLIGHTLAB® non-linear model and frequency response approximations

The baseline isolated rotor model utilized in this analysis is a high fidelity non-linear model that is representative of a UH-60 helicopter rotor implemented in FLIGHTLAB®. The model features finite-element blade representation and a 33-state Peters-He inflow model. FLIGHTLAB® provides the option to incorporate turbulence-induced fluctuations on each blade element at the Aerodynamic Computational Points (ACPs), which are the specific locations where the induced velocity is determined. This serves as the baseline model, with rotor parameters altered to create various configurations.

After trimming the isolated rotor for the specific mean wind speed ($U_0 = 22$ knots), which involves trimming for certain thrust value and zero moments, frequency sweeps are applied to the FLIGHTLAB® non-linear model in order to find the frequency responses. The input (u) and output (y) vectors are chosen as shown in Eqs. (8) and (9), respectively. Figure 4 shows an example of the rotor response when subjected to a sweep of longitudinal input. The data gathered from these input sweeps is then processed using CIFER® to obtain the frequency responses for different inputs and outputs. The on-axis frequency response of the pitch moment coefficient, resulting from the longitudinal input as determined by CIFER®, is depicted in Fig. 5, where the data show high coherence.

$$u = [\theta_0 \ \theta_{1s} \ \theta_{1c}]^T \quad (8)$$

$$y = [C_T \ C_{M_y} \ C_{M_x}]^T \quad (9)$$

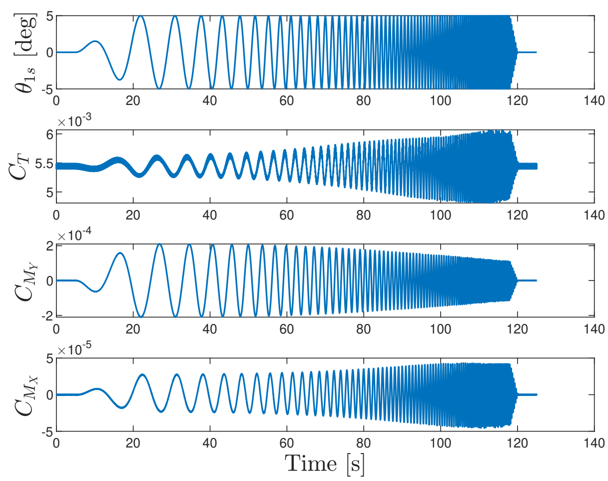

Figure 4. Sweep input to the non-linear model

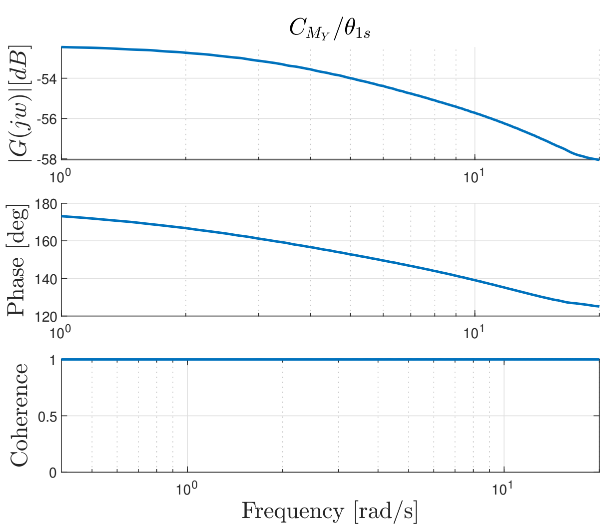

Figure 5. Frequency response of rotor hub pitch moment variations to swashplate longitudinal input C_{M_y}/θ_{1s}

Ranges of Parameters for Design of Experiment

For the ranges of values of the parameters, we examined the characteristics of different rotor configurations from known helicopters. Specifically, we considered both small and large rotorcraft to ensure that a broader range of possible values is covered. Five helicopter configurations were selected for this analysis: the UH-60, OH-6A, BO-105C, UH-1H, and CH-53D. The data for the UH-60 is taken from Ref. 20, while Ref. 21 is used for the other rotorcraft. By examining the main rotors of these vehicles, we established a set of ranges for the dimensional parameters, which in turn informed the resulting values for the non-dimensional parameters. The resulting values for the non-dimensional parameters, derived from the parameters of the different rotors, are presented in Table 1. Based on these values, the selected ranges of parameters are presented in Table 2.

Table 1. Rotor Non-Dimensional Parameters

Helicopter	C_W	Tip Mach number	Solidity	Lock number
UH-60	0.0059	0.65	0.082	7.0
OH-6A	0.0052	0.59	0.055	4.9
BO-105C	0.0048	0.63	0.070	5.0
UH-1H	0.0028	0.72	0.046	6.6
CH-53D	0.0073	0.63	0.115	12.5

Table 2. Range of Values for Non-Dimensional Parameters

Parameter	Minimum Value	Maximum Value
C_W	0.0028	0.0075
Tip Mach number	0.40	0.72
Solidity	0.04	0.12
Lock number	3.5	12.5

Selection of Cases

To develop the parametric RCETI models, we employed Latin Hypercube Sampling (LHS) for generating the simulation cases. LHS is a statistical method that ensures a more efficient exploration of the input parameter space compared to simple random sampling. One of the key advantages of using LHS is its ability to produce a reduced number of cases compared to regular discretization methods. By dividing the range of each input variable into equal probability intervals and ensuring that each interval is sampled only once, LHS provides better coverage of the multi-dimensional parameter space (Ref. 22). This approach is particularly effective in high-dimensional spaces, where it becomes crucial to minimize the number of required simulations while still capturing the variability of the system.

In this study, the input parameters included chord length, rotational speed, radius, nominal thrust, blade second moment of inertia, hinge offset, and the number of blades. Each of these dimensional parameters was sampled independently across its range using LHS. Following the sampling process, we ensured that the combination of the resulting cases adequately covered the range of key non-dimensional parameters, which included solidity, Lock number, tip Mach number, thrust coefficient, and flapping frequency. Combinations of dimensional parameters which results in non-dimensional quantities outside of the range were neglected.

Given the proof-of-concept nature of this study, we focused on covering the parameter space with a minimal number of cases to demonstrate the feasibility of the approach. However, the methodology is designed to be scalable. In practical applications, additional data from different rotor configurations can be incorporated, allowing for more cases to be added as further experimentation or simulations are conducted. This flexibility ensures that the model can be refined and expanded as more data become available.

Utilizing the parameters of the cases obtained through LHS, different rotor models were constructed in FLIGHTLAB® to analyze the effect of atmospheric turbulence. Analysis similar to that conducted on the baseline model was performed to determine the different frequency responses which will be used to find the PSD of required inputs.

Simulation of Atmospheric Turbulence

Various methods for simulating the impact of atmospheric turbulence are presented in the literature (Ref. 2). In earlier research (Ref. 13), we employed the shaping filter technique, which is the most widely used method. This technique facilitates frequency domain analysis to examine turbulence effects on vehicles. Using this method, turbulence fluctuations are assumed uniform across the entire disk, known as the hub-fixed sampling approach. While this approach allowed to include longitudinal and lateral turbulence gradients, it does not account for the effects of rotational sampling on the rotor blades. Thus, similar to the work in Ref. 19, we consider the blade-element sampling of turbulence, where the vertical turbulence fluctuations are allowed to vary both along the longitudinal and lateral axes.

The fluctuations of turbulence are found for the ACP of each blade element on the i^{th} blade as follows: (see (Refs. 23, 24) for details):

$$w(X_i,Y_i) = \sum_{j=1}^{N_1}\sum_{k=1}^{N_2}\sqrt{S_{w_g}(\Omega_{1k},\Omega_{2j})\Delta\Omega_1\Delta\Omega_2}\,\cos(\Omega_{1k}X_i+\Omega_{2j}Y_i+\Phi_{k,j}) \tag{10}$$

where S_{w_g} is the spectrum of vertical turbulence, and $\Phi_{k,j}$ is a random phase angle uniformly distributed over $[0,2\pi]$. The Phase-Randomization is equivalent to exciting the system with a band-limited white noise (Ref. 25). In addition, X_i and Y_i are defined as follows:

$X_i = U_0 t - r\,cos\psi_i$

$Y_i = r\,sin\psi_i$

where ψ_i is the azimuth angle of blade i.

The two-dimensional spectrum of turbulence following the Dryden model is used in the analysis and is expressed as follows (Ref. 26):

$$S_{wg}(\Omega_1,\Omega_2) = \frac{3\sigma_w^2L_w^2}{2\pi}\frac{({\Omega_1}^2L_w^2+{\Omega_2}^2L_w^2)}{\left(1+{\Omega_1}^2L_w^2+{\Omega_2}^2L_w^2\right)^{\frac{5}{2}}} \tag{11}$$

The parameters of turbulence are chosen following one of the flight tests from Lusardi et al. (Ref. 3): mean wind speed of 22 knots ($U_0 = 22$ knots), turbulence intensity of 5.5 ft/s ($\sigma_w = 5.5$ ft/s), and a scale length of 54 ft, which is relevant to flying at low altitudes. A sample velocity fluctuations for a four-bladed rotor using the two-dimensional Dryden spectrum is shown in Fig. 6.

Although the Von-Karman model is generally more accurate and recommended for use when possible (Ref. 1), the Dryden model still yields comparable results and is therefore suitable for our study (Ref. 19). Thus, in the analysis herein, we continue to use the Dryden model for consistency with our previous work (Ref. 13).

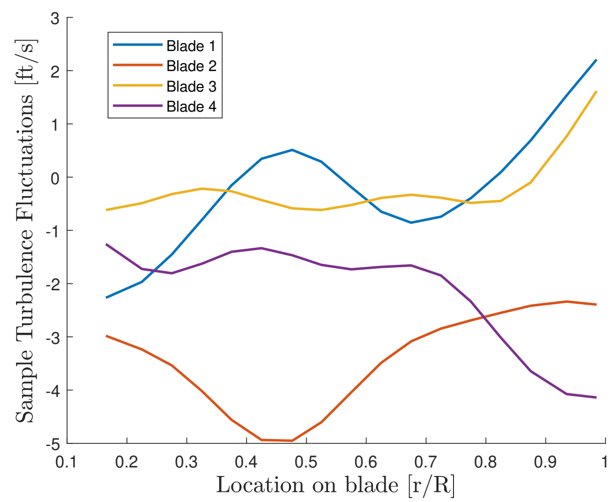

Figure 6. Sample fluctuations of the vertical turbulence found using the two-dimensional spectrum for a four-bladed rotor

Recovering Input Traces

Turbulence fluctuations are found and used as inputs to the ACPs at the blade elements of the FLIGHTLAB® model. Time-domain simulations are conducted and the rotor hub loads are recorded. Using CIFER®, the PSDs of the hub loads due to turbulence are found from the time-domain simulations of the different cases. In the next step, the transfer functions of the hub-loads due to swashplate inputs are used to find the remnant input PSDs that would produce the same response spectrum produced by turbulence (this is done similar to Eq.(7). The work presented in this paper focuses on the results for the collective input θ_0. However, models for $\theta_1 s$ and $\theta_1 c$ parameters could also be developed following the same methodology.

While any shaping filter could be used to match the PSD of the input, it is evident that higher-order filters provide a better fit to the data. To demonstrate this, first, second, and third-order filters were constructed to fit the collective input of the baseline UH-60 rotor, and are shown in Fig. 7. The resulting transfer functions and their associated error functions, as found from Eq. 12, are summarized in Table 3. The first and second order filters yield high error values while the third-order filter yields an error function of 50, which is considered to be low and within acceptable ranges (Ref. 18). Since we will use a Neural Network to create the parametric model, it is important to minimize the error arising from the fit. Therefore, third-order filters are used to fit the data. This way, the output of the Neural Network will consist of the coefficients of a third-order transfer function.

$$J = \frac{20}{n_\omega} \sum_{\omega_1}^{\omega_{n\omega}} \left[\left(|\hat{T}_c| - |T| \right)^2 \right] \tag{12}$$

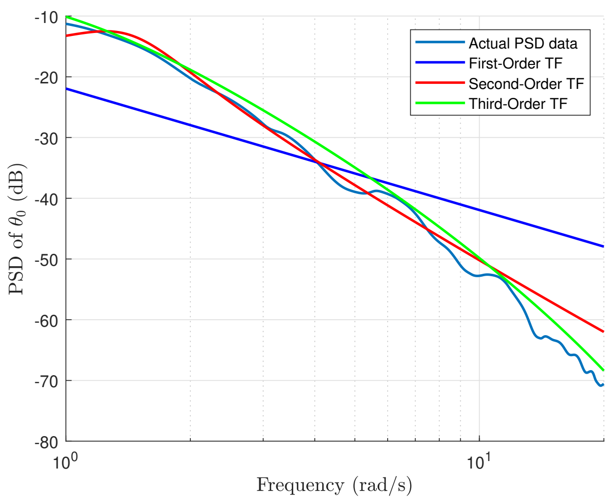

Figure 7. Transfer function fits of PSD values

Table 3. RCETI filters of collective input (θ_0)

Transfer function	Error function J
$\frac{0.08}{s+0.005}$	1960
$\frac{0.005s+0.3}{s^2+0.95s+2}$	180
$\frac{0.003s^2+4.5}{s^3+10s^2+15.2s+7.7}$	50

Developing RCETI filters

Simulations are performed for all cases to determine the PSD of hub load coefficients due to turbulence. Using the frequency responses, PSDs of the required inputs are obtained. Figure 8 illustrates the PSD of the collective input for all cases, showing variability in the results. This indicates the need for developing parametric models. Using CIFER®, third order transfer functions are constructed for all the different rotor configurations. In the following section, a Neural Network is employed to establish the parametric model between the rotor parameters and the coefficients of the third-order transfer function that represents the PSD data.

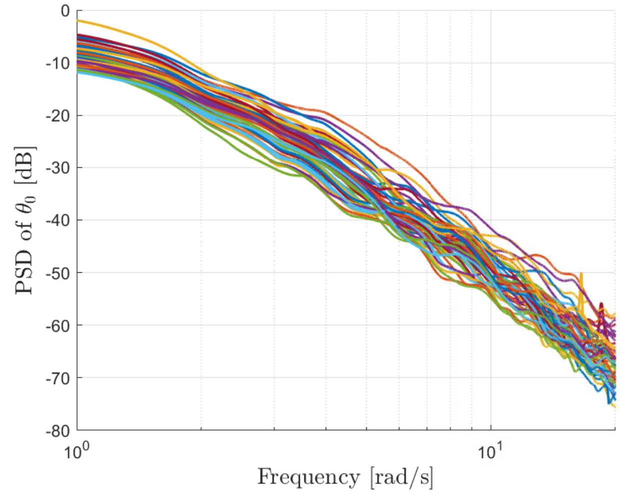

Figure 8. PSD of collective input for different cases

Neural Network Training and Testing

The neural network architecture used in this study is illustrated in Figure 9. The architecture consists of a simple, single-layer cascaded network, chosen due to the moderate complexity of the problem and the limited amount of available data. The input layer is composed of the non-dimensional rotor parameters, while the output layer provides the RCETI filter parameters. The flapping frequency is not used as one of the input parameters for the collective input, since the effect was shown to be negligible in previous work (Ref. 19). The network contains five neurons in the hidden layer, a choice made to balance model complexity and performance. This configuration was considered suitable for the problem, as the relationship between input and output variables did not require highly complex network.

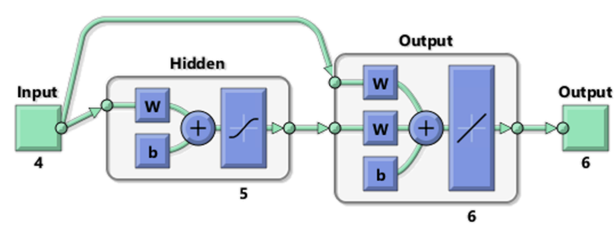

Figure 9. Neural Network Architecture used for RCETI Model Development

The neural network was trained using a set of simulation cases generated through Latin Hypercube Sampling (LHS). The training set covered a broad range of rotor configurations, with the goal of capturing the variability inherent in the rotor response to turbulence. Bayesian regularization, as implemented in MATLAB, was used during training to mitigate overfitting and ensure the model generalizability. The training process involved iterative adjustments of the network weights to minimize the error between the predicted and actual RCETI filter parameters.

The decision to use five neurons in the hidden layer was driven by the complexity of the problem and the size of the training dataset. Since the task is not complex, a small number of neurons was sufficient to achieve an accurate fit. This also helped to reduce the risk of overfitting, particularly given the limited training data. The choice of five neurons was validated by the performance of the model on both the training and testing datasets, which demonstrated that the network was capable of capturing the essential relationship without unnecessary complexity.

After training, the network was tested using a separate set of cases not included in the training set. In this study, three testing cases were analyzed. Figures 10, 11, and 12 show the network performance on selected testing cases. These figures illustrate how well the model generalizes to new data, with the predicted PSD of input closely matching the actual PSD values. The error cost function as in Eq.12 is calculated and presented in the figures, which demonstrates the validity of the model.

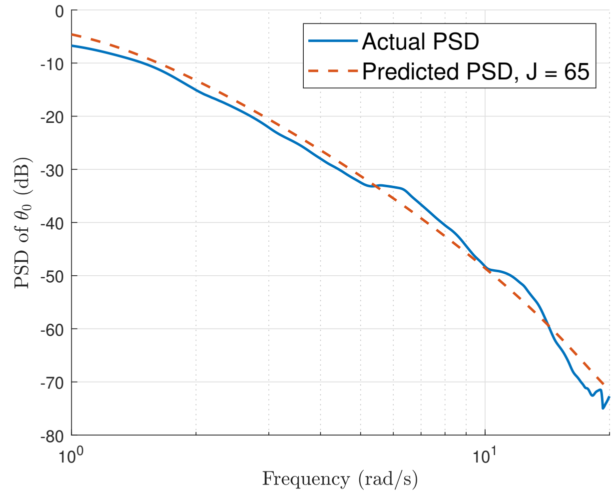

Figure 11. Testing Case 2: Comparison of Predicted vs. Actual PSD for θ_0

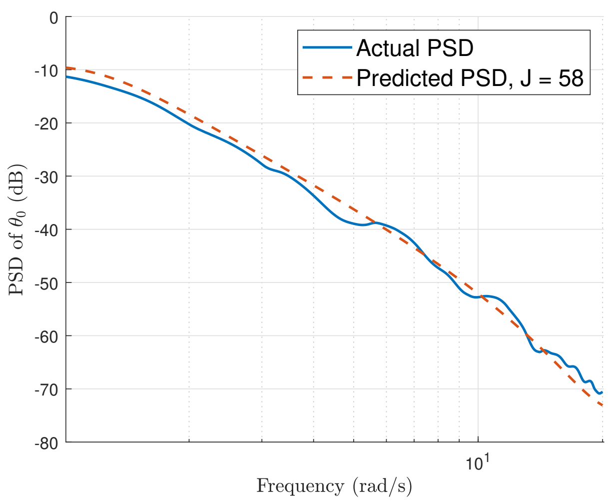

Figure 10. Testing Case 1: Comparison of Predicted vs. Actual PSD for θ_0

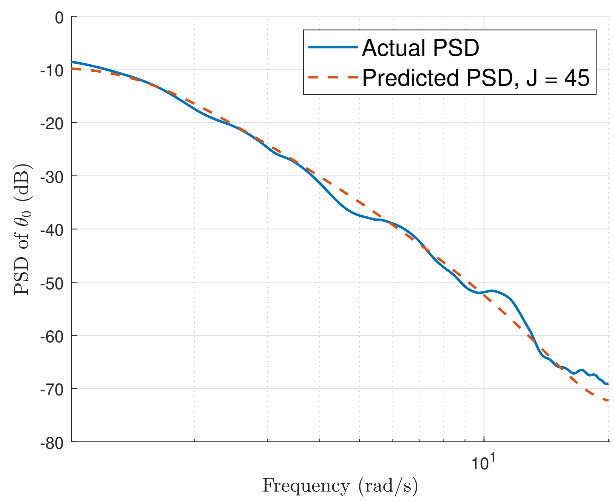

Figure 12. Testing Case 3: Comparison of Predicted vs. Actual PSD for θ_0

These results indicate that the neural network, despite its simple architecture, is effective in generalizing from the training data to unseen cases. The close agreement between the predicted and actual PSD values as well as the low error function across multiple test cases demonstrates the robustness of the model and its potential applicability to a range of rotor configurations.

CONCLUSION

In this work, the concept of Rotor Control Equivalent Turbulence Input is extended to simulate the response of various rotor configurations to two-dimensional spatial turbulence, with the goal of developing parametric RCETI models. RCETI models were developed using CIFER® to match the PSD of required inputs to replicate the response due to turbulence. Different to previous work, the analysis encompasses a broader range of rotor parameters. Moreover, instead of the use of dimensional parameters, non-dimensional parameters have been considered to enhance the generalizability of the models.

Furthermore, neural network modeling have been utilized to create parametric models. In these models, the input consists of the different rotor non-dimensional parameters, while the output is the set of parameters for the RCETI models. The following conclusions can be drawn from this study:

1. Parametric RCETI models can be effectively developed using a simple neural network architecture.
2. Non-dimensional rotor parameters could be used as input to the Neural Network, with the outputs being the coefficients of the RCETI filter.
3. The neural network-based parametric models demonstrate scalability, allowing them to be extended to dif-

ferent rotorcraft configurations beyond those considered in the development.

Future work will include the integration of real test data or CFD data to enhance the fidelity of the models. Additionally, there is potential to expand the approach of developing parametric models for the Control Equivalent Gust Input (CEGI) models, which would focus on deterministic gusts as opposed to continuous turbulence.

Author contact: Mahmoud A. Hayajnh mhayajnh3@gatech.edu, and J.V.R. Prasad jp23@gatech.edu.

ACKNOWLEDGMENTS

This research was partially funded by the U.S. Government under Cooperative Agreement No. W911W6-21-2-0001. The U.S. Government is authorized to reproduce and distribute reprints for Government purposes notwithstanding any copyright notation thereon.

The views and conclusions contained in this document are those of the authors and should not be interpreted as representing the official policies of position, either expressed or implied, of the U.S. Army Combat Capabilities Development Command (DEVCOM), Aviation & Missile Center (AvMC), or the U.S. Government.

REFERENCES

1. Anon., "Flying Qualities of Piloted Aircraft," *Dept. of Defense Interface Standard TR*, , (MIL-STD-1797B), February 2006.
2. Gaonkar, G., "Review of Turbulence Modeling and Related Applications to Some Problems of Helicopter Flight Dynamics," *Journal of the American Helicopter Society*, Vol. 53, January 2008, pp. 87–107.
3. Lusardi, J., Blanken, C., and Tischler, M., "Piloted Evaluation of a UH60 Mixer Equivalent Turbulence Simulation Model," Proceedings of the American Helicopter Society 59th Annual Forum, May 6-8, 2002.
4. Baillie, S. W., and Morgan, J. M., "An In-Flight Investigation into the Relationships Among Control Sensitivity, Control Bandwidth and Disturbance Rejection Bandwidth Using a Variable Stability Helicopter." Proceedings of the 15th European Rotorcraft Forum, Amsterdam, The Netherlands, September 12-15, 1989.
5. Lusardi, J. A., Tischler, M. B., Blanken, C. L., and Labows, S. J., "Empirically Derived Helicopter Response Model and Control System Requirements for Flight in Turbulence," *Journal of the American Helicopter Society*, Vol. 49, (3), July 2004.
6. Lusardi, J., *Control equivalent turbulence input model for the UH-60 helicopter*, Ph.D. thesis, University of California, Davis, January 2004.
7. Seher-Weiss, S., and Grünhagen, W., "Development of EC 135 Turbulence Models via System Identification," *Aerospace Science and Technology - AEROSP SCI TECHNOL*, Vol. 23, December 2012.
8. Seher-Weiss, S., and von Gruenhagen, W., "Development of EC 135 Turbulence Models via System Identification," Proceedings of the 35th European Rotorcraft Forum, Hamburg, Germany, September 22-25, 2009.
9. Juhasz, O., Lopez, M., Berrios, M., Berger, T., and Tischler, M., "Turbulence Modeling of a Small Quadrotor UAS Using System Identification from Flight Data," , January 2017.
10. Juhasz, O., Tischler, M. B., and Won, H., "System Identification and Control Law Optimization Applied to the AeroVironment QuantixTM Tail-Sitter UAS," Proceedings of the AHS International 74th Annual Forum, May 2018.
11. Truong, K., Gong, A., Berger, T., Tischler, M., and Ivler, C., "Development of a Reconfigurable Control Equivalent Turbulence Input Model for Multirotor UAS," Proceedings of the Vertical Flight Society 77th Annual Forum, May 2021.
12. Hayajnh, M. A., and Prasad, J. V. R., "Rotor Control Equivalent Turbulence Input (RCETI) Models," Proceedings of the 48th European Rotorcraft Forum, Winterthur, Switzerland, September 5-8, 2022.
13. Hayajnh, M. A., and Prasad, J. V. R., "Development of Parametric Rotor Control Equivalent Turbulence Input (RCETI) Models for Rotorcraft," Proceedings of the Vertical Flight Society 79th Annual Forum, West Palm Beach, Florida, May 16-18, 2023.
14. Hayajnh, M. A., and Prasad, J. V. R., "Rotor Control Equivalent Turbulence Input (RCETI) Models for Multi-Rotor Vehicles," Proceedings of the 49th European Rotorcraft Forum, Buckeberg, Germany, September 5-7, 2023.
15. Seher-Weiß, S., and Jones, M., "Control Equivalent Turbulence Input Models for Rotorcraft in Hover and Forward Flight," *Journal of Guidance, Control, and Dynamics*, Vol. 44, (8), 2021, pp. 1517–1524.
16. Berger, T., and Lopez, M. J. S., "Frequency Domain Identification of a Multi-Input Control Equivalent Turbulence Input Model," *Journal of Guidance, Control, and Dynamics*, Vol. 45, (1), 2022, pp. 15–27.
17. Julius S. Bendat, A. G. P., *Random Data: Analysis and Measurement Procedures*, Wiley, fourth edition, 2010., Chapter 5.
18. Tischler, M., and Remple, R., *Aircraft and Rotorcraft System Identification: Engineering Methods with Flight Test Examples*, AIAA education series, American Institute of Aeronautics and Astronautics, 2012.

19. Hayajnh, M. A., and Prasad, J. V. R., "Parametric Rotor Control Equivalent Turbulence Input (RCETI) Models for Different Rotor Configurations," Proceedings of the Vertical Flight Society 80th Annual Forum, Montréal, Québec, Canada, May 7-9, 2024.

20. Hilbert, K., *A Mathematical Model of the UH-60 Helicopter*, AVSCOM technical memorandum, Defense Technical Information Center, 1984.

21. Heffley, R., Jewell, W., Lehman, J., and Winkle, R., "A Compilation and Analysis of Helicopter Handling Qualities Data, Volume One: Data Compilation." *NASA Contractor Reports*, August 1979.

22. McKay, M. D., Beckman, R. J., and Conover, W. J., "A Comparison of Three Methods for Selecting Values of Input Variables in the Analysis of Output from a Computer Code," *Technometrics*, Vol. 21, (2), 1979, pp. 239–245.

23. Riaz, J., Prasad, J. V. R., Schrage, D. P., and Gaonkar, G. H., "Technical Notes: Atmospheric Turbulence Simulation for Rotorcraft Applications," *Journal of the American Helicopter Society*, Vol. 38, (1), 1993, pp. 84–88.

24. Jamshed, R., *A simulation model of atmospheric turbulence for rotorcraft applications*, Ph.D. thesis, Georgia Institute of Technology, May 1992.

25. Shinozuka, M., and Jan, C.-M., "Digital simulation of random processes and its applications," *Journal of Sound and Vibration*, Vol. 25, (1), 1972, pp. 111–128.

26. Van Staveren, W., *Analyses of Aircraft Responses to Atmospheric Turbulence*, Ph.D. thesis, Delft University, January 2003.